The International Journal of Engineering and Science (IJES)
|| Volume || 7 || Issue || 5 Ver. II || Pages || PP 34-51 || 2018 ||
ISSN (e): 2319 – 1813 ISSN (p): 23-19 – 1805

Generalization of Calculation Method for Seismic Intensity Using Filtered Acceleration

Akira Sakai
Department of Civil Engineering and Architecture, Saga University, Japan
Corresponding Author' Akira Sakai

ABSTRACT
Most current seismic intensity scales used to express the degree of ground shaking during earthquakes classify the intensity into 12 classes considering observations based on human perception and the behavior of the surroundings, with the exception of the instrumental seismic intensity scale by the Japan Meteorological Agency (JMA), which is based on an instrumental seismic intensity meter. The present study generalizes both the acceleration weighting factor and the seismic intensity formula used as the JMA instrumental seismic intensity and clarifies the relationships among the different seismic intensities obtained using arbitrary seismic intensity parameters. In this paper, previously proposed methods for obtaining the seismic intensities using the velocity and displacement are compared with those obtained using the presently proposed method with various seismic intensity parameters. Additionally, an index that evaluates the extent of the seismic intensity based on the time history is discussed.

KEYWORDS: *seismic intensity, instrumental seismic intensity, seismic intensity level, weighting factor of acceleration*

Date of Submission: 05-05-2018 Date of acceptance: 21-05-2018

I INTRODUCTION

Since April 1996, automatic measurements have been carried out in Japan using instrumental seismic intensity meters to determine the Japan Meteorological Agency (JMA) scale defining ten classes of seismic intensity (JMA, 2009), supersending the conventional manner of observation based on human perception and the behavior of the surroundings. The seismic intensity not only expresses the degree of shaking at each ground surface during earthquakes, but also plays an extremely important role in ensuring each organization requested for relief and urgent activity after an earthquake can act quickly. Thus, determining the seismic intensity just after an earthquake is very useful from the perspective of disaster prevention. Most seismic intensity scales, such as the Modified Mercalli Intensity scale, the Medvedev-Sponheuer-Karnik scale, and the European macroseismic scale, contain twelve classes of intensity, but the seismic intensity is not calculated using a seismic intensity meter. The establishment of a common method of expressing the seismic intensity based on the instant determination of the seismic intensity at each point is desired with the substantiation of the organization responsible for maintaining the observation network in the near future.

This paper proposes a method for expressing the seismic intensity that includes extending the parameters used to calculate the weighted acceleration based on the instrumental seismic intensity and the seismic intensity calculation formula. The original instrumental seismic intensity was proposed on the basis of the Kawasumi formula (Kawasumi, 1943) denoted by an acceleration and used a filter corresponding to the effect of the seismic period. The present instrumental seismic intensity formula (Seismic Intensity Problem Study Committee, 1995), which was improved in 1996, fundamentally conforms with the approach of the original scale. However, in the present formula, the instrumental seismic intensity is considered to mainly correspond to the short-period band up to approximately 1 s to cut the long-period wave through the low-cut filter. It is well known that the seismic intensity does not correspond to the damage to various structures with a wide range of frequency characteristics.

To express the seismic intensity considering the effect of medium or long period (periods greater than 1 s) as well as the combined seismic intensities obtained from velocity and displacement waveforms (Kiyono et al., 1999, 2001), a method using each periodic band of velocity response spectrum (Sakai et al., 2004) and a method based on the velocity response of a single-degree-of-freedom system (Shino, 2010) were proposed. The effective evaluation methods of the long-period seismic motion were also discussed (JMA, 2012). A method of obtaining the seismic intensity level L_{Fs} using the running root mean square (RMS) method, which can express the time history of the seismic intensity, was proposed by the author in a previous study (Sakai, 2012). Seismic intensity levels corresponding to the velocity and displacement were also suggested, and the concern with the filter properties of the instrumental seismic intensity based on acceleration was clarified (Sakai, 2013). In recent years, the long-period ground motion, which has large influence on the shaking of tall buildings and tanks, has attracted

attention, and the JMA has presented four classes of long-period ground motion using the maximum value of the absolute-velocity response spectrum (JMA). The intensity scales of long-period ground motions obtained by changing the weighting factor of the instrumental seismic intensity parameters were proposed based on the assumption of the frequency band related to the first dominant frequency of high-rise buildings (Kanda et al., 2014). The long-period seismic intensity level using the seismic intensity level with the middle quality of velocity and displacement were also proposed by the author (Sakai, 2015). Seismic intensity levels using the parameters of the acceleration weighting factor extended so that the frequency characteristics could be taken into consideration are suggested in this paper, and the relationships among these parameters are clarified. The index of the seismic intensity level is also proposed to express the time-related extent of seismic intensity level.

II SEISMIC INTENSITY CALCULATION METHOD USING ACCELERATION

2.1 Seismic Intensity Filtering

The instrumental seismic intensity I on the basis of the Kawasumi formula uses the filtered acceleration, which considers the effect of the period to conform with the conventional manner of measuring seismic intensity through human perception. The filtered acceleration used to calculate the instrumental seismic intensity was obtained by applying the following three filter functions to the frequency f: (1) a period effect filter, (2) a high-cut filter, and (3) a low-cut filter. The filter functions, which add three parameters f_p, β, and α, were used in this study to express an arbitrary weighting factor for the acceleration, as described by the following equations.

1) Period effect filter: $F_{a1}(f)$

$$F_{a1}(f) = \left(f_p / f\right)^{\beta} \tag{1}$$

2) High-cut filter: $F_{a2}(f)$

$$F_{a2}(f) = \left(\begin{array}{l} 1 + 0.694X^2 + 0.241X^4 + 0.0557X^6 + \\ 0.009664X^8 + 0.00134X^{10} + 0.000155X^{12} \end{array}\right)^{-1/2} \qquad X = f / f_c \tag{2}$$

3) Low-cut filter: $F_{a3}(f)$

$$F_{a3}(f) = \left(1 - \exp(-(f / f_{L0})^3)\right)^{\alpha} \tag{3}$$

where f_{L0} is the lower limit of the frequency used to calculate the seismic intensity. The values of f_p, β, f_c, f_{L0}, and α used in the present instrumental seismic intensity formula are 1 Hz, 0.5, 10 Hz, 0.5 Hz and 0.5, respectively. The total weighting factor $\lambda_a(f)$, which is the product of these three filters, is given as

$$\lambda_a(f) = F_{a1}(f)F_{a2}(f)F_{a3}(f) \tag{4}$$

Figure 1 shows the filter characteristics of the instrumental seismic intensity. The coordinates (f_{peak}, $(\lambda_a(f))_{\max}$) of the maximum weighting factor are 0.625 Hz and 1.17, respectively. The values of the parameters f_p, β, f_c, f_{L0}, and α influence the acceleration weighting factor $\lambda_a(f)$ as a function of the frequency. Figure 2(a)-(d) shows the effect of each parameter on the acceleration weighting factor $\lambda_a(f)$. The maximum weighting factor $(\lambda_a(f))_{\max}$ in Fig.2(a) and (c) increases as the parameter f_p for the period effect increases and the parameter f_{L0} for the low-cut filter decreases. In addition, the gradient of the weighting factor below the frequency at the maximum weighting factor is the same.

Furthermore, the gradient of the weighting factor in the frequency region lower f_{peak} decreases with increasing β and decreasing with α, as shown in Fig.2(b) and (d), whereas the gradient in the frequency region higher than f_{peak} increases with increasing β. The coordinates (f_{peak}, $(\lambda_a(f))_{\max}$) depend on the parameter f_c related to the high-cut filter when f_p is lower than f_c, in which case both the maximum weighting factor $(\lambda_a(f))_{\max}$ and the peak frequency f_{peak} decrease, as shown in Fig.3(a). However, the effect of the high-cut filter $F_{a2}(f)$ on the coordinates (f_{peak}, $(\lambda_a(f))_{\max}$)of the maximum weighting factor is extremely small in the region of $X < 0.2$ because the filter function exceeds 0.986, as shown in Fig.3(b).

Therefore, when $f_p \le 0.2f_c$ the coordinates (f_{peak}, $(\lambda_a(f))_{\max}$) of the maximum weighting factor can be approximately obtained by using the partial weighting factor $\lambda_{a13}(f)$, which is the product of only two filters, the period effect filter $F_{a1}(f)$ and the low-cut filter $F_{a3}(f)$, and is defined as

$$\lambda_{a13}(f) = \left(f_p / f\right)^{\beta}\left(1 - \exp(-(f / f_{L0})^3)\right)^{\alpha} \tag{5}$$

The gradient of the logarithms of the weighting factor $\lambda_{a13}(f)$ with respect to the logarithm of the frequency is defined as

$$\frac{d(\ln \lambda_{a13}(f))}{d(\ln f)} = -\beta + \frac{3\alpha(f / f_{L0})^3}{\exp(f / f_{L0})^3 - 1} \tag{6}$$

The peak frequency f_{peak} can be obtained by setting the gradient in Eq.(6) equal to zero, as

$$-\beta + \frac{3\alpha\left(f_{peak} / f_{L0}\right)^3}{\exp(f_{peak} / f_{L0})^3 - 1} = 0 \tag{7}$$

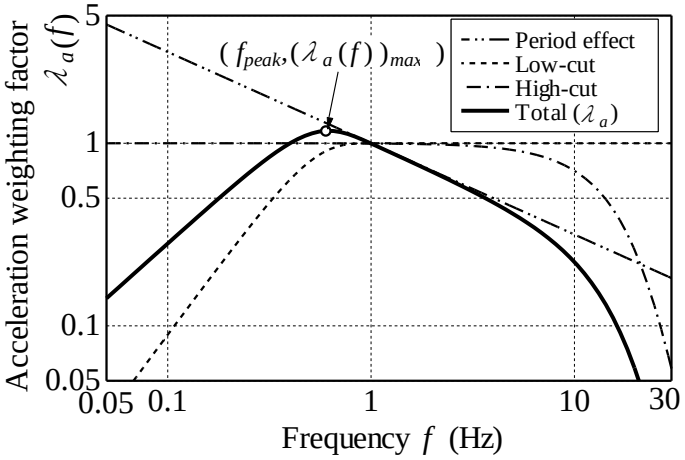

Figure 1: Acceleration weighting factor for the instrumental seismic intensity

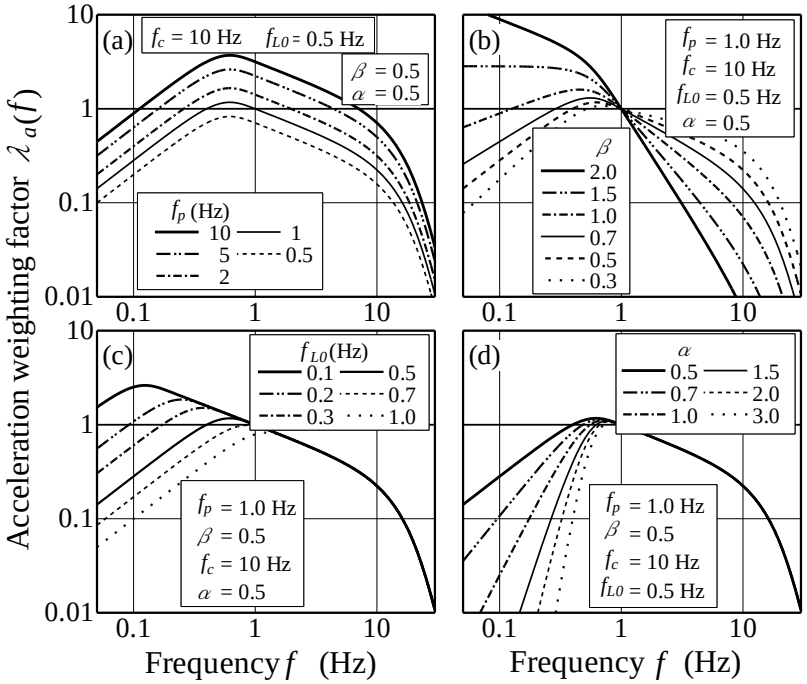

Figure 2: Effects of parameters on weighting factor.

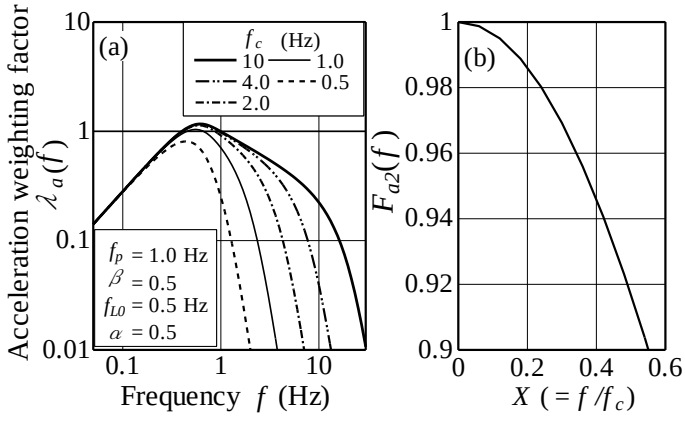

Figure 3: Effect of parameter fc.

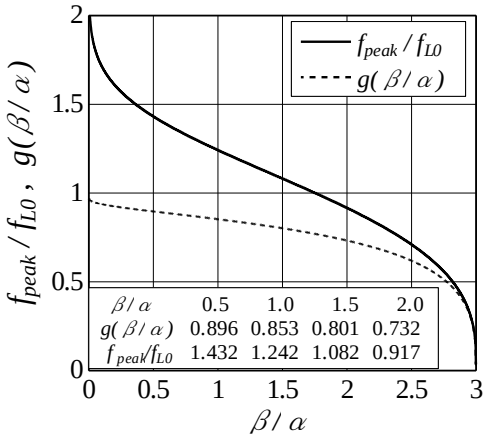

Figure 4: Relationship between f_{peak}/f_{L0} and β/α.

From Eq.(7), f_{peak}/f_{L0} can be expressed as a function of β / α, as shown in Fig.4. Here, f_{peak} exists only when $\beta/\alpha < 3$. The peak weighting factor $\lambda_{a13}(f_{peak})$ is given as follows by substituting Eq.(7) into Eq.(5).

$$\begin{aligned}\lambda_{a13}(f_{peak}) &= \left(f_p / f_{peak}\right)^{\beta}\left(1-\exp(-(f_{peak}/f_{L0})^3)\right)^{\alpha} \\ &= \left(f_p / f_{peak}\right)^{\beta}\left[\left\{1-\exp\left(-\left(f_{peak}/f_{L0}\right)^3\right)\right\}^{\frac{\alpha}{\beta}}\right]^{\beta} \\ &= \left(f_p / f_{peak}\right)^{\beta}\left\{g(\beta/\alpha)\right\}^{\beta}\end{aligned} \tag{8}$$

where

$$g(\beta/\alpha) = \left\{1-\exp\left(-\left(f_{peak}/f_{L0}\right)^3\right)\right\}^{\frac{\alpha}{\beta}} \tag{9}$$

f_p/f_{peak} at an arbitrary $\lambda_{a13}(f_{peak})$ can be obtained from Eq.(8) as

$$f_p / f_{peak} = \frac{\left(\lambda_{a13}(f_{peak})\right)^{1/\beta}}{g(\beta/\alpha)} \tag{10}$$

The gradient n of the weighting factor in the frequency region lower than f_{peak} can be expressed as a function of the parameters α and β because the denominator of the second term in Eq.(6) is approximately $(f/f_{L0})^3$ when the higher-order terms in the Taylor expansion are disregarded. This yields

$$n = 3\alpha - \beta \tag{11}$$

2.2 Acceleration Used in Seismic Intensity Formula

To calculate the seismic intensity, a Fourier transform of acceleration is carried out in three directions, and the Fourier spectrum is revised using the total weighting factor $\lambda_a(f)$, which is defined as the product of the three filters in Eq.(4). The three time histories of the filtered acceleration obtained by the inverse Fourier transform are then synthesized to obtain the vector acceleration $a_w(t)$. The acceleration A used in the seismic intensity formula can be obtained from $a_w(t)$ using the following two methods.

a) Method I: Instrumental seismic intensity method (JMA)

The amplitude of the vector acceleration A used in the instrumental seismic intensity is determined using not the maximum value but the acceleration a_0 corresponding to the accumulated time τ_0 of 0.3 second (JMA). This method uses the value A for the acceleration when the accumulated time for accelerations larger than a_0 is τ_0.

$$A = a_0 \tag{12a}$$

b) Method II: Running RMS method

The running RMS method uses the weighted RMS acceleration $A_w(t)$ based on the vector acceleration $a_w(t)$, which is the sum of the filtered accelerations in the north-south, east-west, and up-down directions. The weighted RMS acceleration is defined as

$$A = A_w(t) = \left(\frac{1}{\tau}\int_{t-\tau}^{t} a_w^2(t)dt\right)^{1/2} \tag{12b}$$

where τ is the integral time of the running average and t is the time.

2.3 Seismic Intensity Formura

The seismic intensity I_{SI} is given by the following equation based on the logarithm of the acceleration value A.

$$I_{SI} = b * \log(A / A_0) \quad (13a)$$

where A_0 is the standard frequency-weighted acceleration at which the seismic intensity equals zero.

When the running RMS method is applied, the calculated seismic intensity is called the seismic intensity level $L_{SI}(t)$ (Sakai, 2013).

$$(L_{SI}(t))_{\max} = b * \log\{(A_w(t))_{\max} / A_0\} \quad (13b)$$

The coefficient b is defined as a function of the acceleration A_k at the seismic intensity k shown in Fig.5 as

$$b = \frac{k}{\log(A_k / A_0)} \quad (14)$$

The instrumental seismic intensity $I = 2\log a_0 + 0.94$ is the formula at $b = 2$, $A_0 = 0.339$ Gal, and $A_7 = 1072$ Gal based on Eqs.(13a) and (14). In addition, the seismic intensity level $L_{Fs}(t) = 2\log A_w(t) + 1.25$ proposed by the author in a previous study (Sakai, 2012), which employs the filtered accelerations obtained using the same filter as the instrumental seismic intensity and an integral time τ of 2 s in Eq.(12b), is the intensity formula at $b = 2$, $A_0 = 0.237$ Gal, and $A_{7.25} = 1000$ Gal when the correlation with $(L_{Fs})_{\max}$ and the instrumental seismic intensity is maximized.

2.4 Influence of Maximum Acceleration Weighting Factor on Seismic Intensity Level

The maximum weighting factors $(\lambda_a(f))_{\max}$ with the same peak frequency f_{peak} depend on the parameter f_p for the period effect, in which the weighting factor $\lambda_a(f)$ increases only to the vertical direction in parallel as the parameter f_p increases, as shown in Fig.2(a). Here, the influence of the $(\lambda_a(f))_{\max}$ value in that case on the seismic intensity level $L_{SI}(t)$ is discussed.

The weighting factor $\lambda_a(f)$ in Eq.(4) can be rewritten in using the period effect filter divided into f_p and f, as

$$\lambda_a(f) = \left\{\left(f_p\right)^{\beta}(f)^{-\beta}\right\}F_{a2}(f)F_{a3}(f) = \left(f_p\right)^{\beta}\lambda_{a0}(f) \quad (15)$$

where $\lambda_{a0}(f)$ is the weighting factor at $f_p = 1$ Hz. The weighted RMS acceleration $A_w(t)$, which is based on the vector acceleration $a_w(t)$ obtained by using the weighting factor $\lambda_a(f)$ in Eq.(15), is expressed as

$$\begin{aligned} A = A_w(t) &= \left(\frac{1}{\tau}\int_{t-\tau}^{t} a_w^2(t)dt\right)^{1/2} = \left(f_p\right)^{\beta}\left(\frac{1}{\tau}\int_{t-\tau}^{t} a_{w0}^2(t)dt\right)^{1/2} \\ &= \left(f_p\right)^{\beta} A_{w0}(t) \end{aligned} \quad (16)$$

where $A_{w0}(t)$ is the weighted RMS acceleration based on the vector acceleration $a_{w0}(t)$ for $f_p = 1$ Hz. Therefore, the seismic intensity level $L_{SI}(t)$ is given as a function of f_p, β, and b as

$$\begin{aligned} L_{SI}(t) &= b * \log\{A_w(t) / A_0\} = b * \log\{(f_p)^{\beta} A_{w0}(t) / A_0\} \\ &= \log\left(f_p\right)^{b\beta} + \left[b * \log\{A_{w0}(t) / A_0\}\right]_{f_p=1} \end{aligned} \quad (17)$$

The seismic intensity level $L_{SI}(t)$ for an arbitrary maximum weighting factor $(\lambda_a(f))_{\max}$ with the same peak frequency f_{peak} differs only the difference value of $\log(f_p)^{b\beta}$, meaning that $L_{SI}(t)$ for the arbitrary $(\lambda_a(f))_{\max}$ can be easily converted from the value of $L_{SI}(t)$ at $f_p = 1$ Hz.

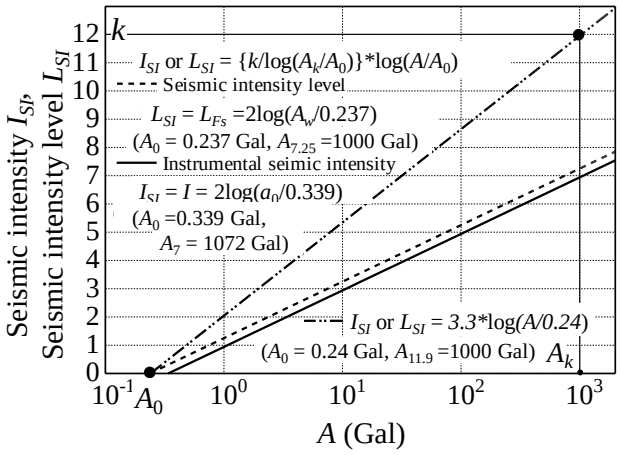

Figure 5: Seismic intensity formula.

III COMPARISONS OF SEISMIC INTENSITIES OBTAINED AT VARIOUS ACCELERATION WEIGHTING FACTORS

3.1 Influence of Acceleration Weighting Factor on Seismic Intensity

The seismic intensity formulas given in Eq.(13a) or Eq.(13b) differ based on the values of the parameters, f_p, β, f_c, f_{L0}, and α. The seismic intensity obtained for five different sets of values for the seismic intensity parameters (Case Nos.1 and 3-6 in Table 1) were compared with the maximum seismic intensity level $(L_{SI})_{\max}$ (Case No.2), which corresponds to the instrumental seismic intensity. The seismic intensity of Case No.1 was set as the instrumental seismic intensity I. The sets of parameter values were selected such that only one parameter in each set differed from the corresponding value in Case No.2. The weighting factors of the seismic intensity parameters in Case Nos.3 and 4 used β = 1.0 and 0.3, respectively, meaning these two cases and Case No.2 each have different gradients of the weighting factor $\lambda_a(f)$ with respect to the frequency, as shown in Fig.2(b). Seismic intensity parameters Nos.5 and 6 use f_{L0} = 0.7 and 0.2, respectively, meaning they have different peak coordinates $(f_{peak}, (\lambda_a(f))_{\max})$, as shown in Fig.2(c).

This study considered seismic waves (NIED) recorded on the ground surface for four earthquakes: the 2011 off the Pacific coast of Tohoku Earthquake (2011 OPCT) (K-NET: 500 points), the 2004 Mid-Niigata Prefecture Earthquake (2004 MNP) (K-NET: 211 points), the 2003 Tokachi-oki Earthquake (2003 TO) (K-NET: 286 points), and the 2016 Kumamoto Earthquake (2016 KM) (K-NET, KiK-net:461 points). Figure 6(a1)-(b2) compares the maximum seismic intensity level $(L_{SI})_{\max} = (L_{Fs})_{\max}$ for No.2 with those $(L_{SI})_{\max}$ for Nos.3-6 at various filtered accelerations for two earthquakes. The maximum seismic intensity level for Nos.3 and 4 in Figs.6(a1) and (b1) was calculated using the weighting factor at which the gradient β of the weighting factor as a function of the reciprocal of the frequency is 1.0 and 0.3, respectively, instead of 0.5 (Case No.2), as shown in Fig.2(b). The maximum seismic intensity level in Case No.4 was approximately equal to or slightly larger than that in Case No.2. Conversely, the maximum seismic intensity level in Case No.3 was larger or smaller than that in Case No.2 because of the difference between the frequency characteristics of these two cases near a frequency of 1 Hz. Figure 6(a2) and (b2) compares the maximum seismic intensity level in Case No.2 with those in Case Nos.5 and 6, which have different f_{L0} values, as shown in Fig.2(c). The seismic intensity level is higher at smaller f_{L0}

Table 1: Parameters used to calculate seismic intensity – 1.

			Instrumental seismic intensity I	Seismic intensity level L_{Fs}	Fig.2(b)		Fig.2(c)	
					β = 1.0	β = 0.3	f_{L0} = 0.7	f_{L0} = 0.2
Seismic intensity parameter number			No.1	No.2	No.3	No.4	No.5	No.6
Acceleration weighting factor	Period effect filter F_{a1}	f_p (Hz)	1.0	1.0	1.0	1.0	1.0	1.0
		β	0.5	0.5	1.0	0.3	0.5	0.5
	High-cut filter F_{a2}	f_c (Hz)	10	10	10	10	10	10
	Low-cut filter F_{a3}	f_{L0} (Hz)	0.5	0.5	0.5	0.5	0.7	0.2
		α	0.5	0.5	0.5	0.5	0.5	0.5
Setting acceleration A	Duration τ_0 (s) (Method I)		0.3	—	—	—	—	—
	Integral time: τ (s) (Method II)		—	2.0				
Seismic intensity formula	b , A_0 (Gal)		2.0, 0.339	2.0, 0.237				

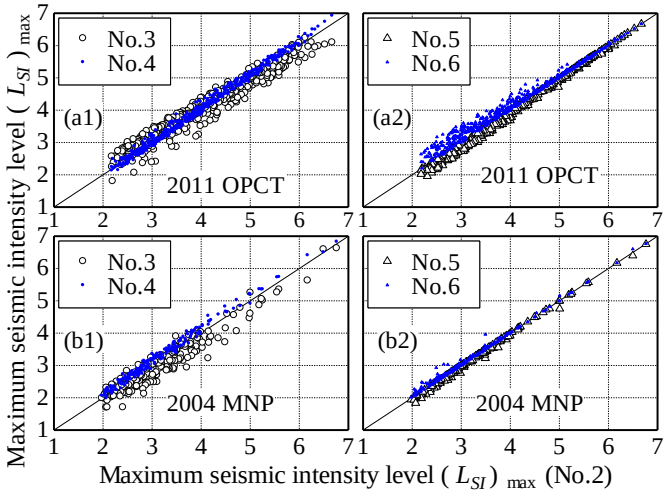

Figure 6: Maximum seismic intensity levels at various filtered accelerations

values, and therefore the Case No.6, which has the smallest f_{L0} value among the three cases, had the greatest seismic intensity level. Similar trends were observed for other earthquakes.

Table 2: Parameters used to calculate seismic intensity - 2.

			Weighting factors (Fig.8)					Weighting factor (Fig.10)		
			L_{Fav}	L_{Fad}	L_{Fap}	L_{Fav}'	L_{Fad}'	(I_{VR})**	(I_{VRS})**	(I_{VRL})**
Seismic intensity parameter number			No.7	No.8	No.9	No.10	No.11	No.12	No.13	No.14
Acceleration weighting factor	Period effect filter F_{a1}	f_p (Hz)	0.714	0.595	0.606	0.714	0.595	1.020	4.869	0.244
		β	1.0	2.0	1.5	1.0	2.0	1.0	1.0	1.0
	High-cut filter F_{a2}	f_c (Hz)	10	10	10	10	10	100	100	100
	Low-cut filter F_{a3}	f_{L0} (Hz)	0.07*	0.07*	0.07*	0.037	0.037	0.647	3.078	0.154
		α	6.0*	6.0*	6.0*	6.0	6.0	0.67	0.67	0.67
Setting acceleration A	Duration τ_0 (s) (Method I)		—	—	—	—	—	0.3	0.063	1.26
	Integral time: τ (s) (Method II)		2.0					—	—	—
Seismic intensity formula	b, A_0 (Gal)		2.0, 0.237					2.0, 0.339	2.0, 0.813	2.0, 0.074
			*Approximate value using f_{L0} and α.					** Approximation		

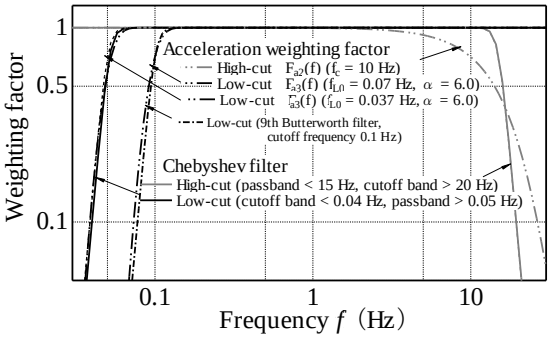

Figure 7: Velocity and displacement weighting factors.

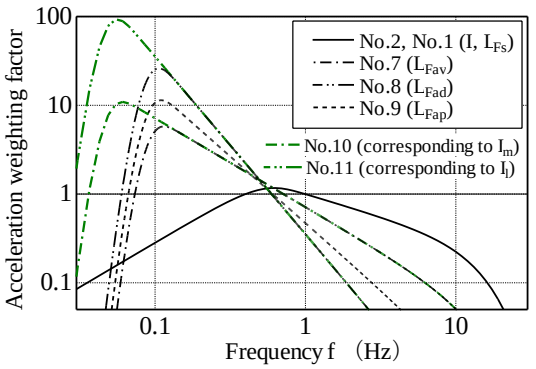

Figure 8: Weighting factors corresponding to velocity and displacement.

3.2 Seismic Intensity Level Corresponding to Velocity and Displacement

It is well known that the instrumental seismic intensity does not correlate with structural damage, such as damage to tall buildings and the sloshing of an oil storage tank with a long primary natural period (JMA,2009). To consider the effects of medium or long period, the combined seismic intensity, which consists of the instrumental seismic intensity I, I_m, and I_l at short, medium, and long periods, was proposed by Kiyono et al. (1999, 2001). The medium-period seismic intensity I_m was calculated using the threshold value v_0 of the vector-filtered velocity at which the total time is 0.3 s after filtering the velocity waveform obtained from the acceleration in three directions, yielding $I_m = 1.91\log(v_0) + 2.50$ (Chebyshev filter: high-cut [passband: 15 Hz, cutoff band: 20 Hz], low-cut [cuoff band: 0.04 Hz, passband: 0.05 Hz]), as shown in Fig.7. The long-period seismic intensity I_l was expressed as a function of the displacement d_0 obtained by applying the same procedure as for I_m to the displacement waveform, which is the integral of the filtered velocity waveform, yielding $I_l = 1.94\log(d_0) + 3.20$.

The velocity and displacement weighting factors $\lambda_{av}(f)$ and $\lambda_{ad}(f)$, which are related to the weighting factor of the instrumental seismic intensity, are given by the following equations using the high-cut filter $F_{a2}(f)$ (f_c = 10 Hz) and the low-cut filter $F_{a4}(f)$ (ninth Butterworth filter with cut-off frequency 0.1 Hz) (Sakai, 2013):

$$\lambda_{av}(f) = (T/T_{av})F_{a2}(f)F_{a4}(f) \quad (18)$$

$$\lambda_{ad}(f) = (T/T_{ad})^2 F_{a2}(f)F_{a4}(f) \quad (19)$$

where T_{av} (= 1.40 s) and T_{ad} (= 1.68 s) are the periods when the period effect filters for $\lambda_{av}(f)$ and $\lambda_{ad}(f)$ are equal to one, respectively. In addition, the weighting factor $\lambda_{ap}(f)$ with intermediate velocity and displacement characteristics was defined as (Sakai, 2015)

$$\lambda_{ap}(f) = (T/T_{ap})^{1.5} F_{a2}(f)F_{a4}(f) \quad (20)$$

where T_{ap} (= 1.65 s) is the period when the period effect filter with intermediate velocity and displacement characteristics is equal to one.

The seismic intensity levels L_{Fav}, L_{Fad}, and L_{Fap}, which use the filtered acceleration $A_w(t)$ with the weighting factors, are given by the same formula as the seismic intensity level L_{Fs}. Here, the weighting factors

$\lambda_{av}(f)$, $\lambda_{ad}(f)$ and $\lambda_{ap}(f)$ can be approximated by the proposed weighting factor $\lambda_a(f)$ (Eq.(4)) without the Butterworth filter $F_{a4}(f)$. The corresponding seismic intensity parameters are those in Case Nos.7-9 in Table 2, and these weighting factors are illustrated in Fig.8. In particular, the weighting factor in the low frequency region can be approximated using the low-cut filter $F_{a3}(f)$ with f_{L0} = 0.07 Hz and α = 6. Moreover, the seismic intensity levels L_{fv} (= 2log$v$* + 2.55) and L_{fd} (= 2log$d$* + 3.54) for the velocity and displacement waveforms can be obtained using the weighted RMS velocity v* and displacement d* using the same high- and low-cut filters as in the instrumental seismic intensity (Sakai, 2013). The maximum intensity levels $(L_{fv})_{\max}$ and $(L_{fd})_{\max}$ are almost the same as the maximum seismic intensity levels $(L_{SI})_{\max}$ ($(L_{Fav})_{\max}$ for Case No.7 and $(L_{Fad})_{\max}$ for Case No.8) corresponding to the velocity and displacement, respectively.

The medium- and long-period seismic intensities I_m and I_l using the Chebyshev filter for the abovementioned four earthquakes are larger than $(L_{SI})_{\max}$ (Case Nos.7 and 8), respectively, as shown in Fig.9(a1) and (b1), because the frequency region in the low-cut filter is wider than that of $(L_{SI})_{\max}$. Here, the weighting factors of L_{Fav}' (Case No.10) and L_{Fad}' (Case No.11) with f_{L0} = 0.037, which have larger peaks than those in Case Nos.7 and 8 using f_{L0} = 0.7, as shown in Fig.8, were more thoroughly evaluated at lower frequencies. The maximum seismic intensity levels $(L_{SI})_{\max}$ for Case Nos.10 and 11 showed a high correlation with I_m and I_l, respectively, as shown in Fig.9(a2) and (b2). Slightly differences of these seismic intensities depend on the gradients 1.91 and 1.94 for I_m and I_l slightly smaller than 2 for $(L_{SI})_{\max}$ in the logarithms for velocity and displacement.

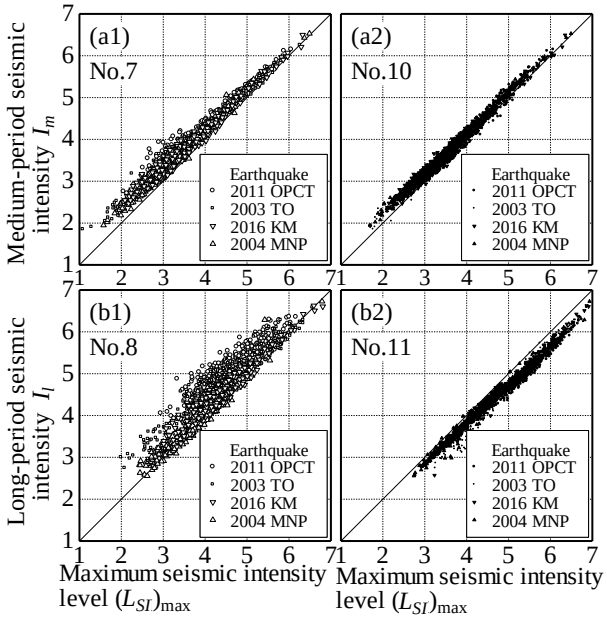

Figure 9: Relationship between I_m, I_l, and $(L_{SI})_{\max}$.

3.3 Comparison between the Velocity Response Seismic Intensity and the Seismic Intensity I_{SI}

The velocity response seismic intensity I_{VR} on the basis of the velocity response of a single-degree-of-freedom (SDOF) system was proposed (Shino, 2010), as one of the seismic intensity for noticing the velocity response, which the frequency response function for the relative velocity of SDOF was similar to the acceleration weighting factor of the instrumental seismic intensity (Case No.1). The amplitude response for I_{VR} was used the natural frequency f_n of 0.7 Hz, the damping ratio h of 0.95, and 10 times value corresponding to the weighting factor of Case No.1, as shown in Fig.10. The amplitude of the frequency response function shows the gradients ±1 with respect to the logarithm of the frequency, and the curve near the natural frequency has a steep shape with decreasing the damping ratio h, such as the broken line when h = 0.3. The acceleration weighting factor of Case No.12 with both the same maximum amplitude response and gradients ±1 in which the seismic intensity parameters β, and α are 1 and 0.67, respectively, from the relation with n=3α-β=1, is drawn as a dash line in Fig.10. Here, the parameter f_c for high-cut filter uses a large value of 100 Hz without affecting the maximum amplitude response. The width of the frequency range in the weighting factor of No.12 has narrowed somewhat because that the curvature is larger than that of I_{VR}.

Furthermore, the short- and long-period velocity response seismic intensity, I_{VRS} and I_{VRL}, were defined by the amplitude response at which f_n, h, and magnification were 3.333 Hz, 0.95, 47.6 times and 0.1666 Hz, 0.95, 2.38 times, respectively, to express the seismic intensity in different frequency ranges in Fig.10. The weighting

factors of Case Nos.13 and 14 show an approximately agreement with the amplitude response for I_{VRS} and I_{VRL}. The velocity response seismic intensities, I_{VR}, I_{VRS}, and I_{VRL} were given by using a threshold value, v_0, v_{S0} , $v_{L0,}$ of the vector velocity for which the total time was τ_0 second, yielding $I_{VR} = 2\log(v_0) + 0.94$, $I_{VRS} = 2\log(v_{S0}) + 0.18$, and $I_{VRL} = 2\log(v_{L0}) + 2.26$. Here, the values of τ_0 for I_{VRS} and I_{VRL} are used not 0.3 s for I_{VR} but 0.063 s and 1.26 s as for $\tau_0 \cdot f_n = 0.3 \times 0.7 = 0.21$. Figure 11(a) and (b) shows a comparison between I_{VR}, I_{VRS}, I_{VRL} and the seismic intensity I_{SI} for Case No.1 (the instrumental seismic intensity I) or Case Nos.12, 13, and 14 for 2011 OPCT. I_{VRS} and I_{VRL} are smaller or larger than that in Case No.1, except for I_{VR}, because of the difference between the frequency characteristics in Fig.10. On the other hand, I_{SI} for Case Nos.12, 13, and 14 are almost the same as I_{VR}, I_{VRS}, and I_{VRL}, respectively, as shown in Fig.11(b).

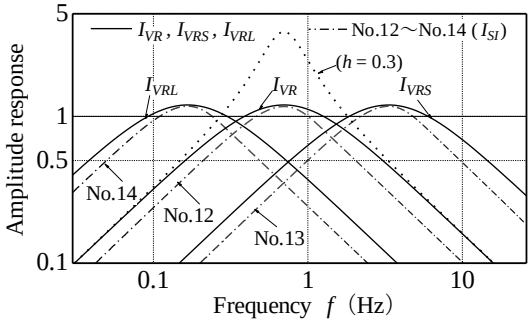

Figure 10: Comparison between amplitude of the frequency response function and the acceleration weighting factors in Case Nos.12-14.

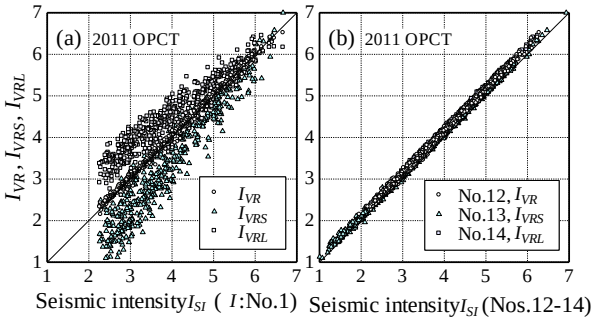

Figure 11: Relationship between ISI and velocity response seismic intensities.

3.4 Seismic Intensities Using Velocity Response Spectrum in Various Period Ranges

The seismic intensity using the velocity response spectrum in arbitrary periodical band is usefull to correspond to the damage for structure with a natural period. As an expression of the seismic intensity depending on the periodical band, three seismic intensities I_L, I_M, and I_H were proposed (Sakai et al., 2004) by using the average velocity response spectra V_L, V_M, and V_H, in the period range of 0.1s-1s, 0.5s-1s and 1s-2s, respectively. These seismic intensities are expressed by the low seismic intensity I_L (=1.936logV_L+2.011), the middle seismic intensity I_M (=2.030logV_M+1.251), and the high seismic intensity I_H (=2.171logV_H+ 1.002). The three velocity average response spectra were assumed: (1) human perception and movement of the indoor article, (2) small or medium-sized damage of the building corresponding to partial or slight destruction, and (3) a great deal of damage of the building corresponding to complete collapse or serious damage. In this study, the relationship between the velocity response spectrum in arbitrary periodical band and the seismic intensity using the acceleration weighting factor will be discussed.

The parameters β and α are first used 1 and 0.67, which show the gradient of ±1 to the frequency as described in 3.3, being able to compare with the velocity response spectrum in arbitrary periodical band from T_1(s) to T_2(s). Also, the coordinates (f_{peak}, $(\lambda_a(f))_{\max}$) of the maximum weighting factor are used a median of the periodical band ($(T_1+T_2)/2=1/f_{peak}$) and 1.17 same as $(\lambda_a(f))_{\max}$ in the instrumental seismic intensity (Case No.1). The parameter f_c for the high-cut filter was set up a value of $1/T_1$ to consider the lower-bound period in the periodical band. The calculation formula of the seismic intensity is same as that of the seismic intensity level L_{Fs} (Case No.2). Table 3 and Figure 12 show the seismic intensity parameter in each periodical band and the acceleration weighting factor used in the paper. These periodical bands are six cases of 0.1~0.5 s (Case No.15), 0.1~1.0 s (Case No.16: V_L), 0.5~1.0 s (Case No.17: V_M), 0.1~2.5 s (Case No.18), 1.0~2.0 s (Case No.19: V_H), 1.6~7.8 s (Case No.20). The coordinates (f_{peak}, $(\lambda_a(f))_{\max}$) has a tendency to gradually decrease with both f_{peak} and $(\lambda_a(f))_{\max}$, when the parameter f_{L0} is approximately more than 20% of f_c, as described in 2.1. Therefore, the parameter f_p except Case No.18 were used a little larger than the value obtained from Eq.(10) to be the same value $(\lambda_a(f))_{\max} = 1.17$. The periodical band of Case No.18 (0.1s~2.5 s) is the same as that of spectrum intensity value (*SI* value). Here, the following equation $SI_{T1\text{-}T2}(h)$ is defined as a value relevant to *SI* value for the velocity response spectrum $S_v(h,T)$ in arbitrary periodical band T_1(s) - T_2(s).

$$SI_{T_1-T_2}(h) = \frac{1}{T_2 - T_1}\int_{T_1}^{T_2} S_v(h,T)dT \qquad (21)$$

Figure 13(a) and (b) shows the comparison between $SI_{T1\text{-}T2}$ at damping ratio h = 5% and the maximum seismic intensity levels $(L_{SI})_{\max}$ using the acceleration weighting factors in Table 3 for the abovementioned four earthquakes. The maximum seismic intensity level $(L_{SI})_{\max}$ in Fig.13(a) has a comparatively high correlation with $SI_{T1\text{-}T2}$ and is small to the same value of $SI_{T1\text{-}T2}$ as the peak frequency f_{peak} in the long-period side, though there is the dispersion in the case of *SI* value (Case No.18) with a wide period range. The relationship between the

maximum seismic intensity levels Case No.16, Case No.17, and Case No.19 corresponding to seismic intensities I_L, I_M, and I_H, and $SI_{T1\text{-}T2}$, as shown in Fig.13(b), shows the same characteristics as the cases in Fig.13(a). Figure 14(a)-(d) shows the comparison between I_L, I_M, and I_H using the velocity response spectra and the instrumental seismic intensity I or the maximum seismic intensity level for Case No.16, Case No.17 and Case No.19. The instrumental seismic intensity I in 2004 MNP in Fig.14(a) has comparatively good correlation with I_L for the periodical band of 0.5 s to 1.0 s and it may be suggested the existence of many observation points having the short predominant period from which I_M and I_H lowers than I. The three seismic intensities I_L, I_M, and I_H in Fig.14(b)-(d) are comparison with the maximum seismic intensity $(L_{SI})_{\max}$ considering the same period range as the average velocity response spectra V_L, V_M, and V_H, respectively. The correlation with $(L_{SI})_{\max}$ has a comparatively good relation, except for I_M indicating the lower value of about 0.5.

Table 3: Parameters used to calculate seismic intensity - 3.

			Period region taken into consideration (Fig.12~Fig.14)					
			(0.1-0.5s)	(0.1-1.0s)	(0.5-1.0s)	(0.1-2.5s)	(1.0-2.0s)	(1.6-7.8s)
Seismic intensity parameter number			No.15	No.16	No.17	No.18	No.19	No.20
Acceleration weighting factor	Period effect filter F_{a1}	f_p (Hz)	5.05*	2.68*	2.22*	1.124	1.12*	0.318*
		β	1.0	1.0	1.0	1.0	1.0	1.0
	High-cut filter F_{a2}	f_c (Hz)	10	10	2	10	1	0.625
	Low-cut filter F_{a3}	f_{L0}(Hz)	3.078	1.682	1.229	0.712	0.619	0.194
		α	0.67	0.67	0.67	0.67	0.67	0.67
Setting acceleration A	Duration τ_0 (s) (Method I)		—	—	—	—	—	—
	Integral time: τ (s) (Method II)		2.0					
Seismic intensity formula	b, A_0 (Gal)		2.0, 0.237					
			*a little larger than the calculated value f_p					

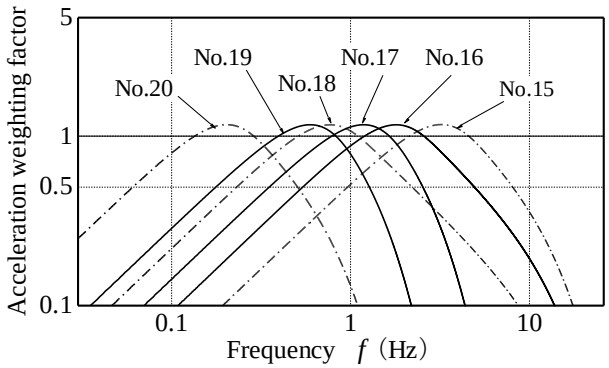

Figure 12: Weighting factor of acceleration withvarious periodical bands.

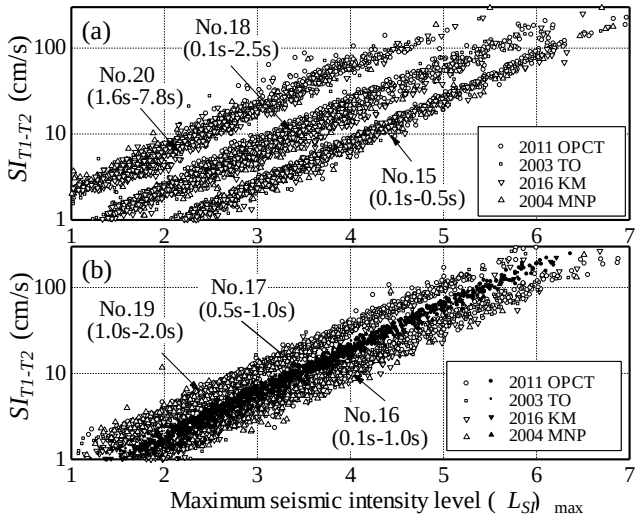

Figure 13: Relationship between $(L_{SI})_{\max}$ and $SI_{T1\text{-}T2}$.

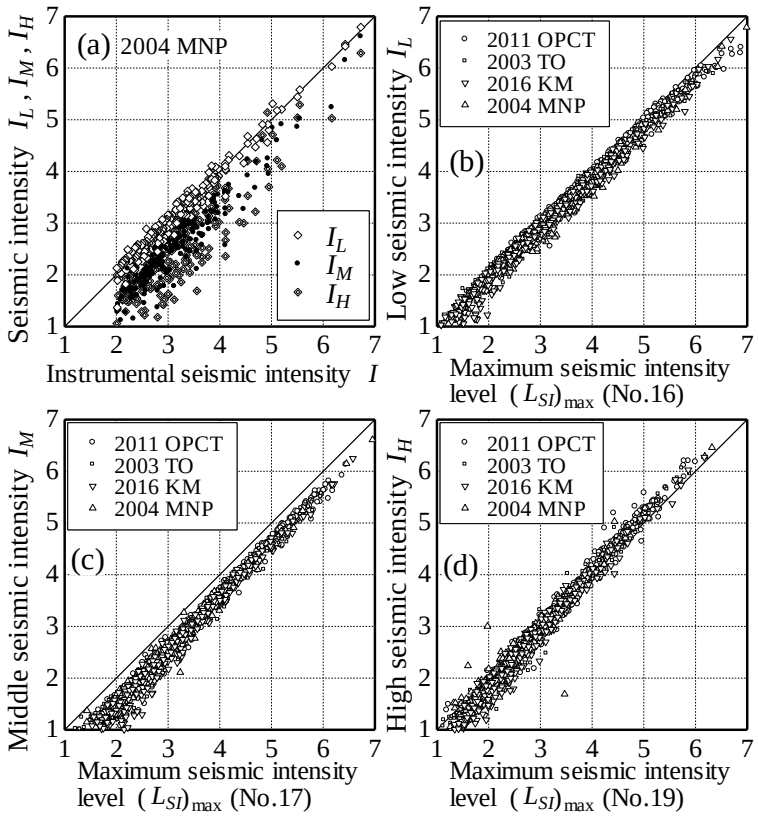

Figure 14: Relationship between I_L, I_M, I_H and I, $(L_{SI})_{max}$.

3.5 Seismic Intensity Level for Long Period Ground Motion

The long-period ground motion scale of the Japan Meteorological Agency is divided into four stages as long-period indices, from the behavioral difficulties of a person to the damage caused by migration and fall such as fixtures and furnitures, etc., in high-rise buildings during a natural period from almost 1.5 to 8 seconds. The value for the scale division uses the maximum absolute velocity response spectrum $(S_v)_{max}$ (h=5%) in the period of 1.6 to 7.8 seconds, which is obtained from the observation data of the seismograph installed on the ground. The boundary values of $(S_v)_{max}$ in each class are 5 cm/s, 15 cm/s, 50 cm/s, and 100 cm/s. The long-period seismic intensity level, which used the maximum seismic intensity level $(L_{Fav})_{max}$ corresponding to velocity , is proposed by the author (Sakai, 2015), from the long-period ground motion acceleration waveform (Ministry of Land, Infrastructure, Transport and Tourism, 2010) (Kozo Keikaku Engineering, 2012). The long-period seismic intensity level using a seismic intensity level with the intermediate characteristics of velocity and displacement is proposed by the author as a new expression of seismic intensity for the long-period ground motion through the clarification of the relation of the $(S_v)_{max}$ with the average value of the velocity response spectrum for the wider period of 1.6 to 7.8. The relationship between the maximum velocity response spectrum $(S_v)_{max}$ and the maximum seismic intensity level, etc., are investigated by the similar method with increasing the reference points from 11 to 1069, in the paper. Two subduction-zone earthquakes, the assumed Tokai Earthquake (M_w8.0) and the assumed Tonankai Earthquake (M_w8.1), are dealt with as object earthquakes (Ministry of Land, Infrastructure, Transport and Tourism, 2010). The acceleration waveform for these earthquakes is calculated about 1300 seconds at intervals of 0.02 second. As for the analysis time, the waveform for 600 seconds in the first half of the acceleration waveform is used.

Figure 15 shows the relationship between the various maximum seismic intensity levels $(L_{Fs})_{max}$, $(L_{Fav})_{max}$, $(L_{Fad})_{max}$, $(L_{Fap})_{max}$ and the maximum velocity response spectrum $(S_v)_{max}$ (h=5%) for the reference points with the period of $(S_v)_{max}$ over 8 seconds in which the long-period feature remarkably appears. Here, the maximum seismic intensity level $(L_{Fap})_{max}$ is obtained by using the weighting factor $\lambda_{ap}(f)$ which indicates the intermediate characteristic of velocity and displacement in Table 2 (No.9). The relationship of the maximum velocity response spectrum $(S_v)_{max}$ and the maximum seismic intensity level $(L_{Fav})_{max}$ corresponding to velocity was already given by the author (Sakai, 2015).

The relationship of the maximum velocity response spectrum $(S_v)_{max}$ (h=5%) with the period of over 8 seconds and the maximum seismic intensity level $(L_{Fav})_{max}$ is rewritten by more additional reference points as shown in Fig.15.

$$\ln(S_v)_{\max} = -1.76 + 1.17(L_{Fav})_{\max} \quad (22)$$

The maximum seismic intensity levels $(L_{Fad})_{\max}$ and $(L_{Fap})_{\max}$ corresponding to displacement and intermediate characteristic of velocity and displacement, respectively, may be expressed by using $(L_{Fav})_{\max}$, although the dispersion is seen somewhat.

$$(L_{Fad})_{\max} \cong (L_{Fav})_{\max} + 1.0 \quad (23)$$

$$(L_{Fap})_{\max} \cong (L_{Fav})_{\max} + 0.5 \quad (24)$$

In order to correspond to the long-period ground motion scale of the JMA using $(S_v)_{\max}$, a maximum long-period seismic intensity level $(L_{Lv})_{\max}$ corresponding to velocity using the maximum seismic intensity level $(L_{Fav})_{\max}$ is first defined by the power function of the following equation.

$$\begin{aligned}(L_{Lv})_{\max} &= c\{(L_{Fav})_{\max}\}^d \\ &= c\{(\ln(S_v)_{\max} + 1.76)/1.17\}^d\end{aligned} \quad (25)$$

where the coefficients of c and d can be obtained by the least squares method using the value of (5,1), (15,2), (50,3), and (100,4) corresponding to the value of $((S_v)_{\max}, (L_{Lv})_{\max})$ in the long-period ground motion scale of the JMA. The coefficients of c and d are 0.132 and 2.0, respectively, and the correlation coefficient is 0.996. Therefore, the maximum long-period seismic intensity level $(L_{Lv})_{\max}$ is given by the following equation using $(L_{Fav})_{\max}$ or $(S_v)_{\max}$.

$$(L_{Lv})_{\max} = 0.132 * \{(L_{Fav})_{\max}\}^2 \quad (26a)$$

$$(L_{Lv})_{\max} = 0.096 * \{\ln(S_v)_{\max} + 1.76\}^2 \quad (26b)$$

The long-period seismic intensity level L_{Lv} corresponding to velocity may be given using the seismic intensity level L_{Fav} as well as $(L_{Lv})_{\max}$ of Eq.(26a) in the following equation.

$$L_{Lv} = 0.132 * (L_{Fav})^2 \quad (27)$$

The long-period seismic intensity level L_{Ld} corresponding to displacement is given by Eq.(23) as follows:

$$L_{Ld} = 0.132 * (L_{Fad} - 1.0)^2 \quad (28)$$

The effect of the long-period ground motion on the evacuation behavior, the uneasy feelings of humans and the overturning/slipping of furniture, etc. in high-rise buildings may be dependent on the response to not only the velocity but also the displacement. Therefore, the seismic intensity level L_{Fap} having the intermediate characteristics of velocity and displacement is used for the long-period seismic intensity level L_{Lp} as follows:

$$L_{Lp} = 0.132 * (L_{Fap} - 0.5)^2 \quad (29)$$

The maximum velocity response spectrum $(S_v)_{\max}$ used as the long-period ground motion scale of the JMA is compared with the maximum long-period seismic intensity level $(L_{Lp})_{\max}$ and $(L_{Lv})_{\max}$, $(L_{Ld})_{\max}$ corresponding to velocity and displacement, as shown in Figure 16. The solid line in the figure expresses the

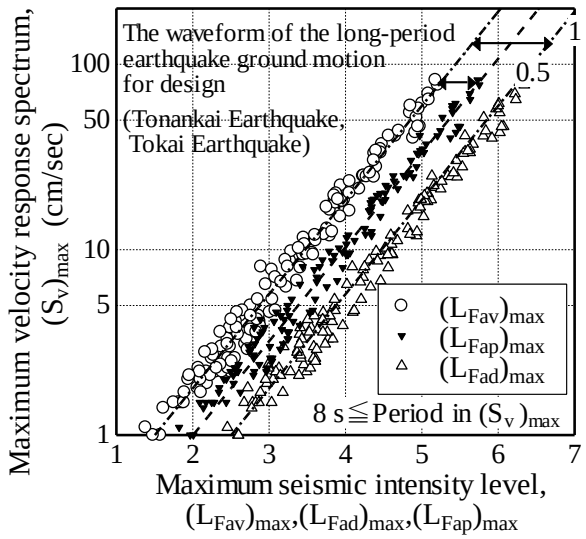

Figure 15: Relationship between the maximum seismic intensity levels and $(S_v)_{max}$.

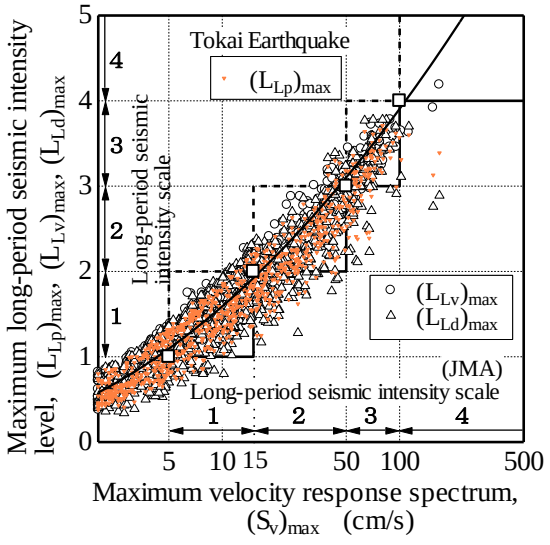

Figure 16: Relationship between the long-period seismic intensity scale and the maximum long-period seismic intensity level.

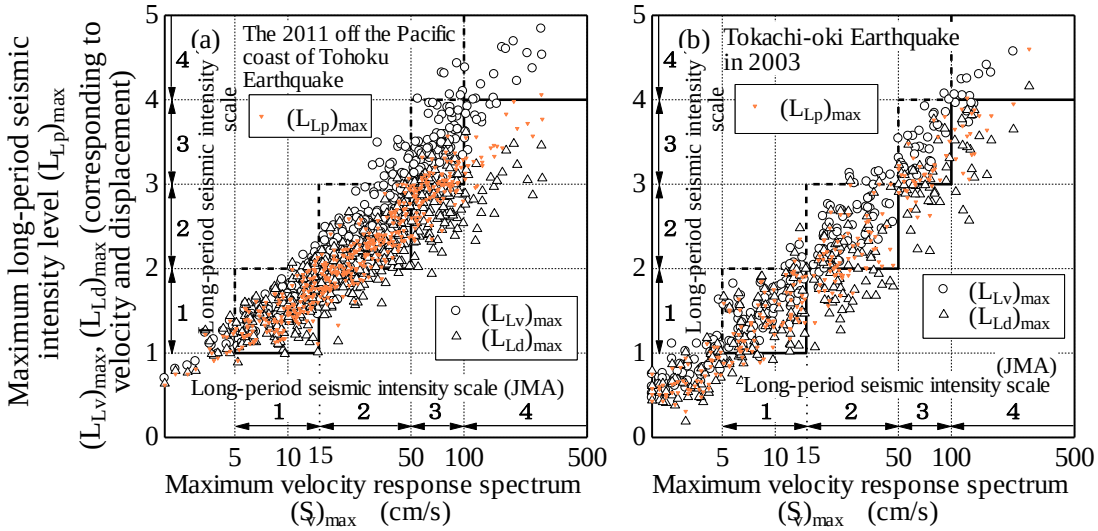

Figure 17: Relationship between the maximum velocity response spectrum and the maximum long-period seismic intensity level.

relation of $(S_v)_{max}$ and $(L_{Lv})_{max}$ in Eq.(26b), and the maximum long-period seismic intensity level $(L_{Lv})_{max}$ is almost the same as the scale of the JMA. The long-period ground motion scale using the maximum seismic intensity level $(L_{Lp})_{max}$, however, includes the points having one class lower than that of the JMA scale, because that the value of $(L_{Lp})_{max}$ in the case of the shorter period for $(S_v)_{max}$ tends to be smaller than that of $(L_{Lv})_{max}$. Figures 17(a) and 17(b) show the relationship between the maximum velocity response spectrum $(S_v)_{max}$ and the maximum long-period seismic intensity levels $(L_{Lp})_{max}$, $(L_{Lv})_{max}$, and $(L_{Ld})_{max}$ in both the 2011 off the Pacific Coast of Tohoku Earthquake and the Tokachi-oki Earthquake in 2003. The maximum long-period seismic intensity level $(L_{Lv})_{max}$ shows almost the same class of the JMA, though the observation points showing the smaller or larger class near the boundary of the long-period ground motion scale exist to some extent. In contrast to $(L_{Lv})_{max}$, the maximum long-period seismic intensity level $(L_{Ld})_{max}$ shows a value lower than that of the class of the JMA in many observation points. Especially, the lowering of two classes is found in the maximum velocity response spectrum $(S_v)_{max}$ of 50 cm/s or more. The long-period ground motion scale used in the long-period seismic intensity level $(L_{Lp})_{max}$ in the paper indicates an intermediate value of $(L_{Lv})_{max}$ and $(L_{Ld})_{max}$, and is one class smaller than that of the JMA scale for the larger $(S_v)_{max}$ region in many observation points.

IV TIME HISTORY AND INDEX OF SEISMIC INTENSITY LEVEL

4.1 Time History of Seismic Intensity Level with Various Acceleration Weighting Factors

The time history of the instrumental seismic intensity cannot be expressed because of the index using the amplitude of the vector acceleration corresponding to a duration of 0.3 s. The calculation of the instantaneous instrumental seismic intensity *IISI* for an arbitrary time window τ is proposed as a method of expressing the time history of the seismic intensity (Kuwata et al., 2002). The fluctuation of *IISI* gradually decreases with increasing time window τ, and the peak value ultimately approaches the instrumental seismic intensity. In a previous study, the author noted that *IISI* agrees moderately well with the instrumental seismic intensity for a time window of 2 s or more (Sakai, 2012). However, the maximum seismic intensity level tends to decrease with increasing integral time τ when using the running RMS method, and no rapid change or constant value was observed after the maximum instantaneous instrumental seismic intensity $(IISI)_{max}$ was reached (Sakai, 2012).

The time histories of the seismic intensity levels L_{SI} for Case Nos.2, 7, and 8, which correspond to the instrumental seismic intensity, velocity and displacement, respectively, are compared in Figure 18(a) and (b). The two observation locations considered here are Funehiki (FKS008) and Misawa (AOM011) for 2011 OPCT, which the spectrum in the long period region was large at Misawa in the Fourier acceleration spectrum, as shown in Fig.18(c1) and (c2). The relationships among the seismic intensity levels L_{Fs}, L_{Fav}, and L_{Fad} of Case Nos. 2, 7, and 8, change with the frequency characteristics of the input seismic waves. The maximum seismic intensity levels $(L_{Fav})_{max}$ and $(L_{Fad})_{max}$ at Funehiki, which appeared at the same time as $(L_{Fs})_{max}$ (Case No.2), were smaller than $(L_{Fs})_{max}$, as shown in Fig.18(a1); this was determined from the fact that the amplification of the acceleration at medium and long periods was not large when the period of the seismic wave was predominantly in the short period region. The largest seismic intensity level in Fig.18(b) was L_{Fs} (Case No.2), followed by L_{Fav} (Case No.7) and L_{Fad} (Case No.8), because of the influence of the peak spectrum at a period of 3.5 s in the long period region, as shown in Fig.18(c2). Furthermore, the time at which the peak value occurred for both L_{Fav} (Case No.7) and L_{Fad} (Case No.8) was approximately 50 s later than that of L_{Fs} (Case No.2).

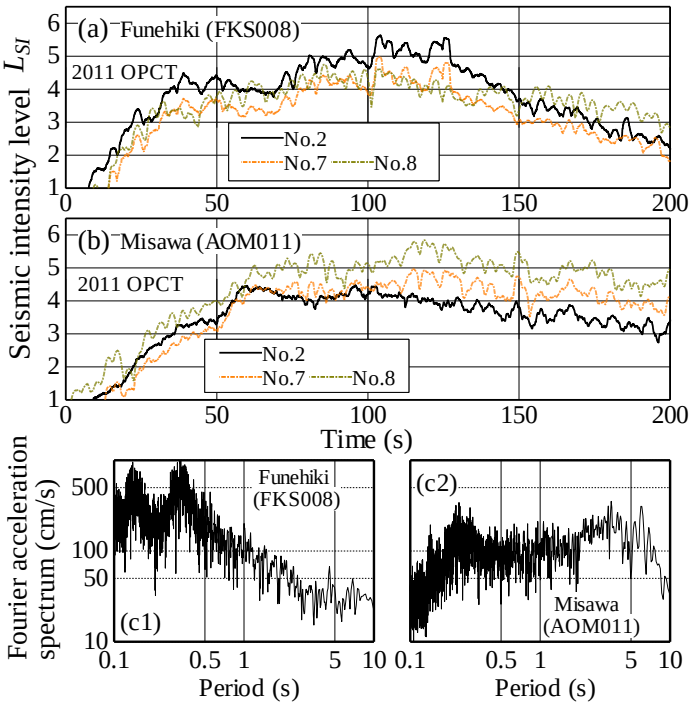

Figure 18: Time histories of seismic intensity levels L_{SI} for Nos.2, 7, and 8 and Fourier spectrum of acceleration.

4.2 Seismic Intensity Level Index I_{SL}

The seismic damage by the ground shaking during earthquake will also receive the influence of the time-related extent of the seismic intensity level as well as the degree of the maximum seismic intensity, so that it may be guessed from Fig.19 showed the difference of the time histories of seismic intensity levels L_{Fs} with the same maximum value. In a previous paper, the author proposed the use of the seismic intensity level index I_{SL}, which is defined as a function of the area of the region surrounded by a seismic intensity level exceeding an arbitrary seismic intensity level $(L_{SI})_i$, using the time history expression of the seismic intensity level. In the present study, the following equation redefines the seismic intensity level index $(I_{SL})_i$ for $(L_{SI})_i$ to allow the comparison of different seismic intensity formulas as shown in Fig.20:

$$(I_{SL})_i = log_{10}\left(\frac{1}{k\Delta t_0}\int_{t_1}^{t_2}(L_{SI}-(L_{SI})_i)dt\right) \qquad (30)$$

where t_1 and t_2 are the initial and final times at which the seismic intensity level L_{SI} is larger than $(L_{SI})_i$, and Δt_0 is one second as a standard time.

Figure 21(a) shows the relationship between the seismic intensity level index I_{SL} and the arbitrary seismic intensity levels $(L_{Fs})_i$ at interval of 0.05 in four cases with the same value of $(L_{Fs})_{max}$ for the two earthquakes, 2011 OPCT and 2016 KM. The seismic intensity k in Eq.(14) was set to 7.25 at an acceleration A_k of 1000 Gal. The seismic intensity level index I_{SL} at each $(L_{Fs})_i$ increases with decreasing of $(L_{Fs})_i$. The 2011 OPCT with a wide-ranging extension on the time history of L_{Fs} shows the seismic intensity level index I_{SL} larger than the case of 2016 KM, as shown also from Fig.21(b) that expressed the relation with the seismic intensity level ratio R_{SI}. Here, the seismic intensity level ratio R_{SI} is a ratio of an arbitrary seismic intensity level $(L_{SI})_i$ and the maximum seismic intensity level $(L_{SI})_{max}$ as

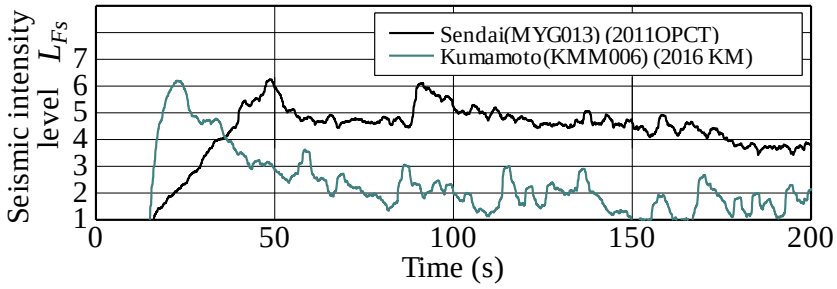

Figure 19: Time histories of seismic intensity levels L_{Fs} with the same maximum value.

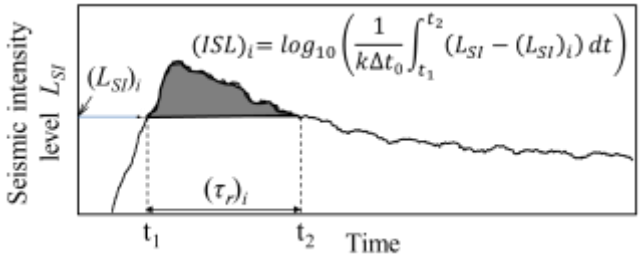

Figure 20: Schematic diagram of the seismic intensity level index $(I_{SL})_i$.

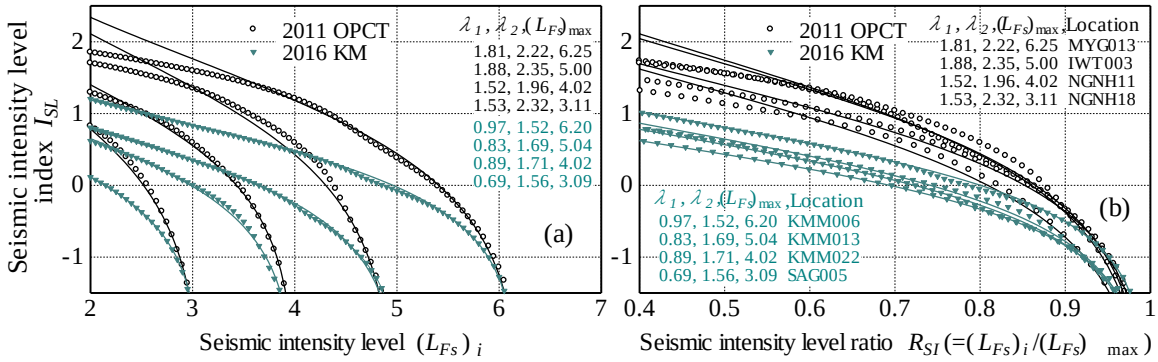

Figure 21: Relationship between arbitrary seismic intensity level $(L_{Fs})_i$, seismic intensity level ratio R_{SI}, and seismic intensity level index I_{SL}.

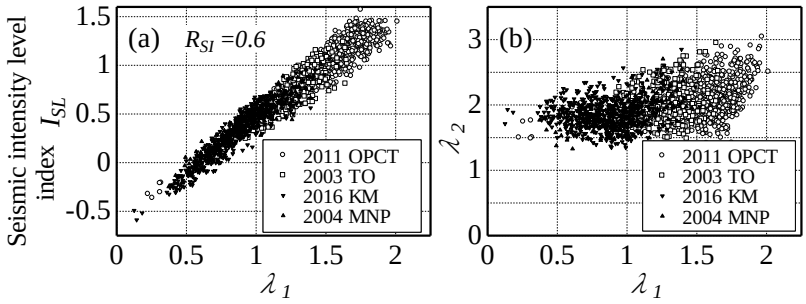

Figure 22: Relationship between λ_1, λ_2 and seismic intensity level index I_{SL}.

$$R_{SI} = \frac{(L_{SI})_i}{(L_{SI})_{\max}} \qquad (31)$$

From these observation results, the approximate seismic intensity index I_{SL} can be obtained from the seismic intensity level ratio R_{SI} as

$$I_{SL} = \log_{10}\left\{\left(\frac{10}{R_{SI}}\right)^{\lambda_1}(1-R_{SI})^{\lambda_2}\right\} \qquad (32)$$

where λ_1 and λ_2 are parameters related to the time history of the seismic intensity level. The seismic intensity level index I_{SL} using Eq.(32), which is expressed in two parameters λ_1, λ_2 obtained from the seismic intensity level ratio R_{SI} of 0.9 and 0.6 for the above-mentioned earthquakes, indicates almost the same value at the ratio R_{SI} ranging over 0.5 as shown in Fig.21. From that the seismic intensity level index I_{SL} is not high correlation with two parameters λ_1, λ_2 as shown in Fig.22, a new parameter λ^* (= λ_1 - $\lambda_2{}^{0.5}$) is introduced as a parameter with a high correlation. Figure 23 shows the relationship between the parameter λ^* and the seismic intensity level index I_{SL}. The parameter λ^* is proportional to I_{LSL} at R_{LSI} of 0.6 though is seen the dispersion at the other values. The seismic intensity level index I_{SL} is expressed with a function of R_{SI} and λ^* as follows:

$$I_{SL} = h_1(R_{SI}) + h_2(R_{SI})\lambda^* \qquad (33)$$

where $h_1(R_{SI})$ and $h_2(R_{SI})$ are a value of I_{SL} at $\lambda^* = 0$ and an incline of straight line in each R_{SI}, respectively. The values of $h_1(R_{SI})$ and $h_2(R_{SI})$ are given by a function of R_{SI} as shown in Fig.24.

When the region in which the seismic intensity level L_{SI} is larger than the arbitrary seismic intensity level $(L_{SI})_i$ expands, λ^* increases, meaning λ^* may be used as an index to evaluate the time-related extent of the seismic

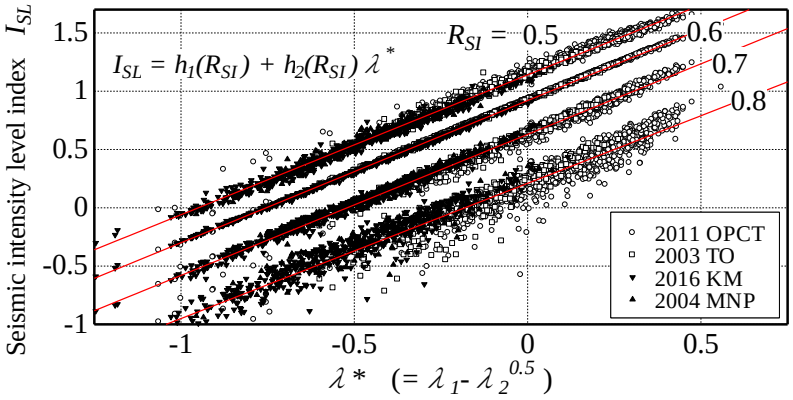

Figure 23: Seismic intensity level index I_{SL} and parameter λ^*.

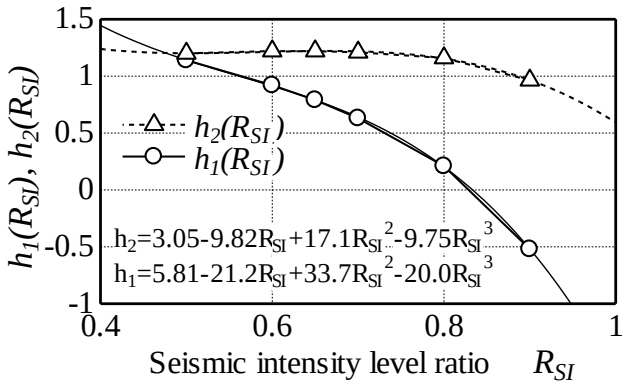

Figure 24: Prameters h_1, h_2 given as a function of R_{SI}.

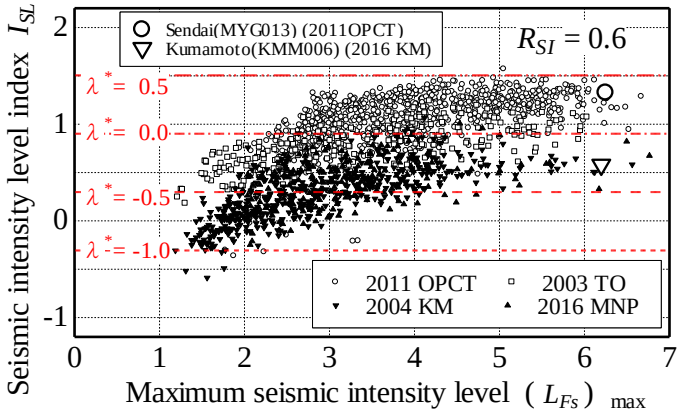

Figure 25: Relationship between $(L_{Fs})_{max}$ and I_{SL}.

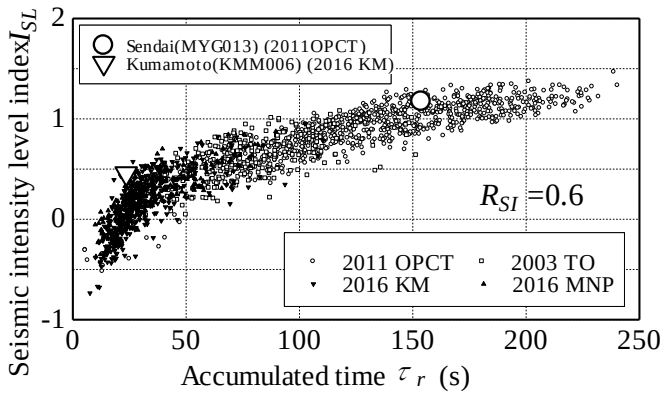

Figure 26: Relationship between accumulated time τ_r and I_{SL}.

intensity level. Figure 25 shows the relationship between the maximum seismic intensity level $(L_{Fs})_{\max}$ and the seismic intensity level index I_{SL} at R_{SI} of 0.6 for the four earthquakes. The seismic intensity level indices I_{SI} against $(L_{Fs})_{\max}$ in 2011 OPCT and 2003 TO of a plate-type earthquake are larger than that in 2016 KM and 2004 MNP of a epicentral earthquake, because of a long duration time that is the acculumated time when the seismic intensity level L_{Fs} is larger than $(L_{Fs})_i$ at $(R_{SI})_i$ in the time history as shown in Fig.26. From these relationships, the typical difference of the time-related extent of the seismic intensity in these two-types of earthquake may be divided on the boundary of near duration time τ_r of 120 seconds and near the seismic intensity level index I_{SL} of 1.0 at R_{SI} = 0.6.

V CONCLUSION

A generalization calculation method for seismic intensity based on the instrumental seismic intensity was proposed, and the relationships between the new seismic intensity parameters and various seismic intensities were clarified. The main results of this study are as follows.

1) The proposed acceleration weighting factor for seismic intensity added three parameters to that for the instrumental seismic intensity, and can be obtained easily by utilizing the relation between the peak value and the parameter for the weighting factor. The formula for the seismic intensity is expressed by the seismic intensity I_{SI} and the seismic intensity level L_{SI} defined using the acceleration value A, which can be obtained using one of two methods: the instrumental seismic intensity and the running RMS methods.
2) The relativity with the proposed weighting factor of acceleration and various seismic intensity expressions which have been suggested by several researchers was clarified as follows. The combined seismic intensities from a velocity waveform and a displacement waveform correspond to the seismic intensity level in extending the frequency region of the weighting factor for the seismic intensity level corresponding to velocity and displacement. The velocity response seismic intensity based on velocity response of a single-degree-of-freedom system is equivalent to the seismic intensity using the weighting factor which does not take a high-cut filter into consideration. The three seismic intensities with average velocity response spectra in the low, middle and high period range correspond with the seismic intensity level by using the weighting factor of acceleration in consideration of these period ranges. The long-period ground motion scale using the maximum velocity response spectrum can be expressed by the seismic intensity level corresponding to velocity.
3) The seismic intensity level index, which is defined as a function of the area of the region surrounded by the time history of the seismic intensity level exceeding an arbitrary seismic intensity level, is expressed as a function of the seismic intensity level ratio and the parameter λ^* that can be used as an index to evaluate the time-related extent of the seismic intensity level.

REFERENCES

[1]. Japan Meteorological Agency , Tables explaining the JMA seismic intensity scale, 2009. http://www.jma.go.jp/jma/en/Activities/inttable.html
[2]. H. Kawasumi, Seismic intensity and seismic intensity scale, *Journal of the Seismological Society of Japan*, 15, 1943, 6-12. (in Japanese)
[3]. Japan Meteorological Agency : Calculation method of instrumental seismic intensity, http://www.seisvol.kishou.go.jp/eq/kyoshin/kaisetsu/calc_sindo.htm (in Japanese)
[4]. Seismic Intensity Problem Study Committee : The final report of seismic intensity problem study committee, 1995. (in Japanese
[5]. Japan Meteorological Agency and Fire and Disaster Management Agency : The report of study committee concerning the seismic intensity, 2009.3. (in Japanese)
[6]. J. Kiyono, K. Fujie, and Y. Ohta, A combined instrumental seismic intensity -concept, formulation and application-, *Doboku Gakkai Ronbunshuu*, 612/I-46, 1999, 143-151. (in Japanese)
[7]. J. Kiyono, K. Toki, T. Usuda, and Y. Ohta, Engineering characterization of instrumental seismic intensity and importance of introducing multi-valued seismic intensity, *Doboku Gakkai Ronbunshuu*, 682/I-56, 2001, 267-278. (in Japanese
[8]. Y. Sakai, T. Kanno, and K. Koketsu, Proposal of instrumental seismic intensity scale from response spectra in various period ranges, *Journal of Structural and Construction Engineering* (Transactions of AIJ), 585, 2004, 71-76. (in Japanese)
[9]. I. Shino, Seismic intensity based on velocity response of single-degree-of-freedom system, *Doboku Gakkai Ronbunshuu A*, 66(4), 2010, 863-873. (in Japanese)
[10]. Japan Meteorological Agency (Seismological and Volcanological Department) : The report of the treatment of information on the long-period ground motion, 2012.3. (in Japanese)
[11]. A. Sakai, A proposal of seismic intensity level using the running r.m.s. method, *Doboku Gakkai Ronbunshuu A*, 68(3), 2012, 673-682. (in Japanese)
[12]. A. Sakai, A method of expressing seismic intensity for a wider period range, *Journal of JSCE*, l, 2013, 262-275.
[13]. Japan Meteorological Agency : The long-period ground motion scale and tables explaining the long-period ground motion scale. (in Japanese) http://www.seisvol.kishou.go.jp/eq/ltpgm_explain/about_ level.html
[14]. K. Kanda, M. Abe, Y. Suzuki, H. Fujiwara, N. Morikawa, T. Maeda, N. Koshika, H. Okano, and K. Kato, Intensity scales of long-period ground motions correlated with structural responses of high-rise buildings, *Journal of Structural and Construction Engineering, Architectural Institute of Japan*, 79(696), 2014, 267-274. (in Japanese)
[15]. A. Sakai, An expression of the seismic intensity level for long-period ground motion, *Journal of JSCE*, 3, 2015, 160-173.
[16]. National Research Institute for Earth Science and Disaster Prevention (NIED), Strong-motion seismograph networks (K-NET) http://www.kyoshin.bosai.go.jp/

[17]. Y. Kuwata, and S. Takada, Instantaneous instrumental seismic intensity and evacuation, *Journal of Natural Disaster Science*, 24(1), 2002, 35-42.
[18]. Kozo Keikaku Engineering Inc. : The software for the long-period ground motion seismic wave evaluation "ARTEQ-LP for Windows Version 1.0", 2012.
[19]. Ministry of Land, Infrastructure, Transport and Tourism : Tentative measures of long-period ground motion in high-rise buildings, etc., 2010. (in Japanese)

Akira Sakai." Generalization of Calculation Method for Seismic Intensity Using Filtered Acceleration " The International Journal of Engineering and Science (IJES) 7.5 (2018): 34-51